Prevention of the Surface Cracks by New High Basicity Mold Powders with Ideal Balance between Softer Heat Removal in Initial Stage and Sufficient Total Heat Removal in the Mold

Junya ITO*1 Shogo YAMASHITA*2
Yukimasa IWAMOTO*3 Daisuke KATAYAMA*4

Abstract

Generally, high basicity mold powders (CaO/SiO_2=1.1−1.4) have been used to cast medium and peritectic carbon steel. However, longitudinal surface cracking can still be an issue. Because softer heat removal in the mold meniscus area is required to prevent surface cracking, the crystallization properties of mold powder slags with higher basicity (>1.5) was investigated. A new very high basicity powder was developed using the results of our own unique slag film simulator. This new mold powder provides softer heat removal in the meniscus area. This new technology improved steel surface quality and provided sufficient solidified shell thickness when used in actual casting.

1. Introduction

In the steel continuous casting process, mold powder is added to surface of the molten steel as it passed through a water-cooled mold. Heat from the molten steel in the mold initiates the melting of the powder, resulting in the presence of a layer of un-melted powder resting upon a layer of molten slag. The molten slag fills the gap between mold and solidified steel shell by the forces of mold oscillation, dragging by the steel shell, and gravity. Molten slag in the gap forms a slag film with a thickness of about 1mm to 2mm. The slag film eventually exits through the bottom of mold. During this process, mold powder provides several essential functions including the prevention of re-oxidation of the steel, thermal insulation, absorption of inclusions, mold lubrication, and heat removal control for improved steel quality and stable casting operation.

A crystal layer is formed in the slag film beside the mold wall during cooling, and it provides resistance to heat transfer from the steel shell to the mold wall. The heat removal in the mold greatly influences the solidification behavior of the steel and the strand surface quality. Optimization of the heat removal is one of the most important roles of mold powder development.

Strand surface cracks when casting peritectic and medium carbon steel grades in carbon range 0.08% to 0.18% are caused by uneven solidification of the steel shell due to the $\delta \rightarrow \gamma$ phase transformation that is accompanied by high solidification shrinkage[1]. Uneven solidified shell in the initial stage easily causes depressions, deep oscillation marks, and several kinds of cracks on the strand surface because the thinner shell thickness can result in local areas of high stress. Strand surface cracks are more likely to occur with high speed casting and/or high alloy content grades[2].

In order to make a uniform solidified shell, an effective and common method is to have softer heat removal in the mold with increased heat resistance in the slag film. The mold powder development for the prevention of surface cracks on medium carbon grades has been active since the 1980s. Multiple investigations on higher basicity (CaO/SiO_2) powders, in the range of 1.1 to approximately 1.4, indicate that as the formation of Cuspidine ($3CaO-2SiO_2-CaF_2$) increases, a crystallization temperature that more likely to yield softer heat removal is reported. This technique has become a popular practice when

*1 Staff Manager, Mold Powder R&D Sec., Research Dept. No.3, Research Center
*2 Mold Powder R&D Sec., Research Dept. No.3, Research Center
*3 General Manager, Mold Powder R&D Sec., Research Dept. No.3, Research Center
*4 Technical Manager, Shinagawa Advanced Materials Americas, Inc.

formulating mold powders[3-9]. After that, further developments that increased/optimized basicity[10,11] and focused on crystallization speed[12,13] were conducted. However, as of today, those technologies have not yielded improved steel quality or operational improvements. Thus, it was necessary to develop new, more effective mold powder technologies and evaluation methods.

The conventional method of increasing crystallization temperature with higher basicity can increase the effect of softer heat removal. However, this could also lead to problems at high speed casting speeds due to lack of lubrication from insufficient liquid layer thickness in the slag film, insufficient shell thickness, and bulging of the strand. In addition, it is possible that further reduction in heat removal with increased crystallization temperature might be difficult in many casting situations, including slow speed casting. This is because almost all conventional mold powder products have already maximized the crystallization temperature which can maintain both lubrication and heat removal.

According to the above background, authors understood that softer heat removal, particularly in the meniscus area where the uneven solidification occurs, is effective in improving strand surface quality. It is assumed that softer heat removal early in meniscus area can be achieved by increasing the heat resistance with quick crystallization as mold powder slag flows into the gap between the mold wall and the solidified shell. In this investigation, optimization of the chemical composition and basicity for crystallization were considered based on a newly developed slag film simulation test. Testing results were then used to develop a new high basicity mold powder for the medium carbon grades, where the crystal layer formation rate is increased due to its higher basicity (over 1.5) composition.

2. Experimental

2. 1 Experimental method

Fig.1 shows a schematic image of the slag film simulation test that has been developed. The mold powder sample was melted in a platinum crucible in an electric furnace, and then a water cooled stainless steel pipe was dipped into the molten slag. The stainless pipe is attached to a motor lift, and oscillation movement was added. The water cooled stainless pipe simulated the water cooled mold of a caster, and the simulation test can

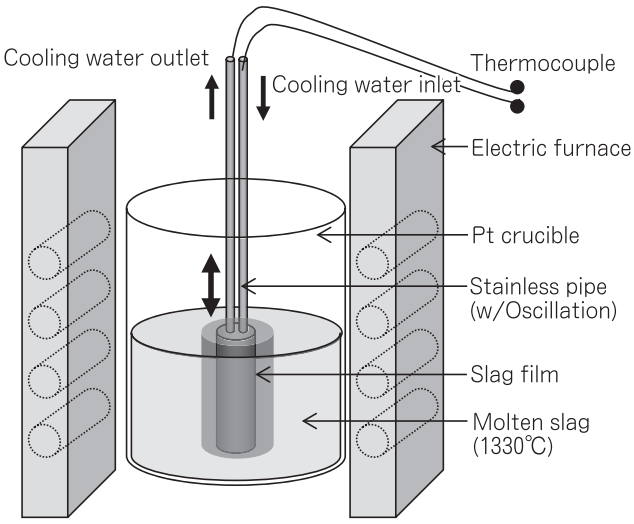

Fig.1 Schematic image of slag film simulator.

yield conditions that the powder slag would experience in the mold. In addition, heat flux measurement and evaluation are available, because each inlet and outlet water temperature of the cooling water can be measured by thermocouples in this system.

The test was performed with a molten slag temperature at 1330 degree C in a ϕ86×140mm platinum crucible. The stainless pipe diameter was 10mm, and it was dipped into the molten slag to a depth of 40mm from the surface. Oscillation movement was set at ±4mm stroke and 100 cycles per minute frequency.

Dipping times were specified for 10, 30, 60, and 180 seconds. The stainless pipe was pulled up from molten slag bath after each dipping time. The slag film that formed around the pipe surface was collected for appearance and cross section observations, and the crystal layer thickness was measured. In addition, a polished surface of the crystal layer structure was observed by optical microscope, and the crystal was identified by X-ray diffraction.

The water flow rate in the stainless pipe was fixed at 600ml·min^{-1} (10^{-5}m^3·s^{-1}), and the inlet and the outlet temperature were measured continuously with thermocouples.

Seven grades of differing basicity mold powder samples were used for the test. Characteristics of the samples are listed in Table 1. In order to evaluate the effect of basicity on slag crystallization, the Fluorine content was fixed in

Table 1 Specifications of mold powder samples

Mold Powder Sample	A	B	C	D	E	F	G
Basicity (CaO/SiO_2)	1.14	1.25	1.45	1.48	1.55	1.55	1.64
F / mass%	12.0	12.0	11.3	11.7	10.6	10.0	12.3
Crystallization Temp. / ℃	1080	1100	1195	1195	1200	1125	1210
Viscosity at1300℃ / Pa•s	0.06	0.06	0.08	0.08	0.09	0.08	0.08

a range from 10mass% to 12mass% to allow Cuspidine crystallization in each sample. These mold powder samples also adjusted the viscosity range within 0.06Pa·s to 0.09Pa·s by changing other chemical compositions in attempt to eliminate the effect of the slag viscosity in the test.

In theory, crystallization temperature is increased as basicity goes up, however, sample F was intentionally designed to have a lower crystallization temperature by adjusting the other components.

2. 2 Experimental result

Fig.2 shows the appearance of the slag film formed on the stainless pipe surface. At a dipping time of 10 seconds, the slag films of Samples A, B, C, and D with basicity in the range of 1.14 to 1.48, were primarily glassy, whereas that of Samples E, F and G with basicity ≥1.55

Fig.2 Characteristics of test samples and slag film appearances.

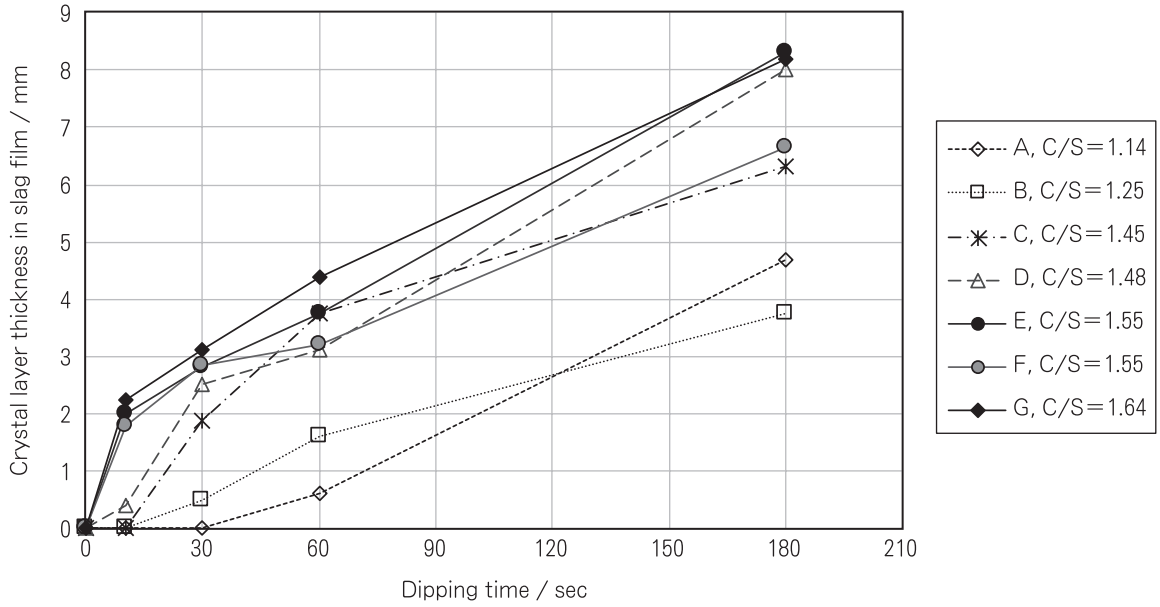

Fig.3 Average crystal layer thickness in slag films (20mm depthposition, C/S=basicity).

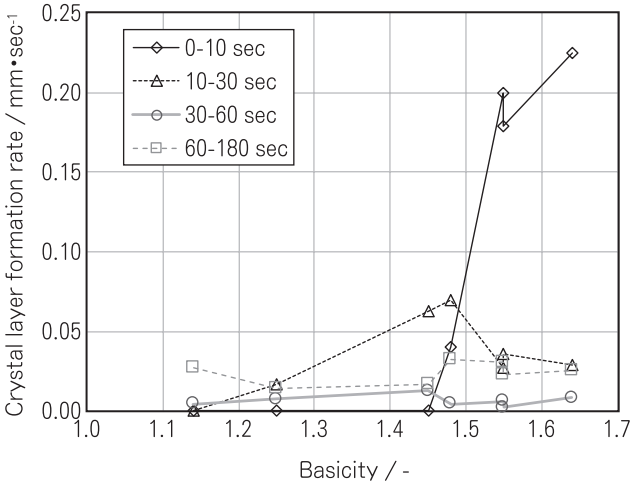

Fig.4 Crystal layer formation rate.

were entirely crystalline. At a dipping time of 30 seconds, the slag films of Samples C, D, E, F, and G with basicity ≥1.45 were entirely crystalline. When the dipping time was increased to 60 seconds, the slag films with basicities ≥1.45 again all formed the crystal phase. Furthermore, when the dipping time was 180 seconds, the slag films of Samples A to G were entirely crystalline.

Fig.3 shows average crystal layer thickness at 20mm depth position for each of the slag films. The Samples E, F and G, with basicities ≥1.55, demonstrated an obviously crystalline layer in the slag film for a dipping time of 10 seconds. Furthermore, when the dipping time was increased to 30 seconds, the thickness of the crystal layer of the high basicity samples tended to be substantial. The difference of slag film thickness formation gradient in the samples in 60 to 180 seconds dipping times was smaller than that of the data in 0 to 60 seconds. From the results of Samples E and F with basicity of 1.55, the slag film thickness for dipping times of 60 seconds or more was increased as the crystallization temperature increased. Thus, the degree of crystal layer thickness formation after 60 seconds was decreased by lower crystallization temperature.

Fig.4 shows the crystal layer formation rate calculated by the time-dependent change of the crystal layer thickness. The crystal layer formation rate for a dipping time 0 to 10 seconds tended to be increased when the basicity was over 1.48. For the dipping time 10 to 30 seconds, the crystal layer formation rate for basicities of 1.45 and 1.48, which displayed low crystallization at 0 to 10 seconds, were increased. At the dipping time from 30 to 180 seconds, no definite influence of basicity on the crystal layer formation rate was observed. In addition, it was determined from the XRD analysis results that the crystals formed in all of slag film samples were primarily Cuspidine.

To evaluate the heat removal properties of each sample, Fig.5 shows the heat flux Hf [$W \cdot m^{-2}$] calculated

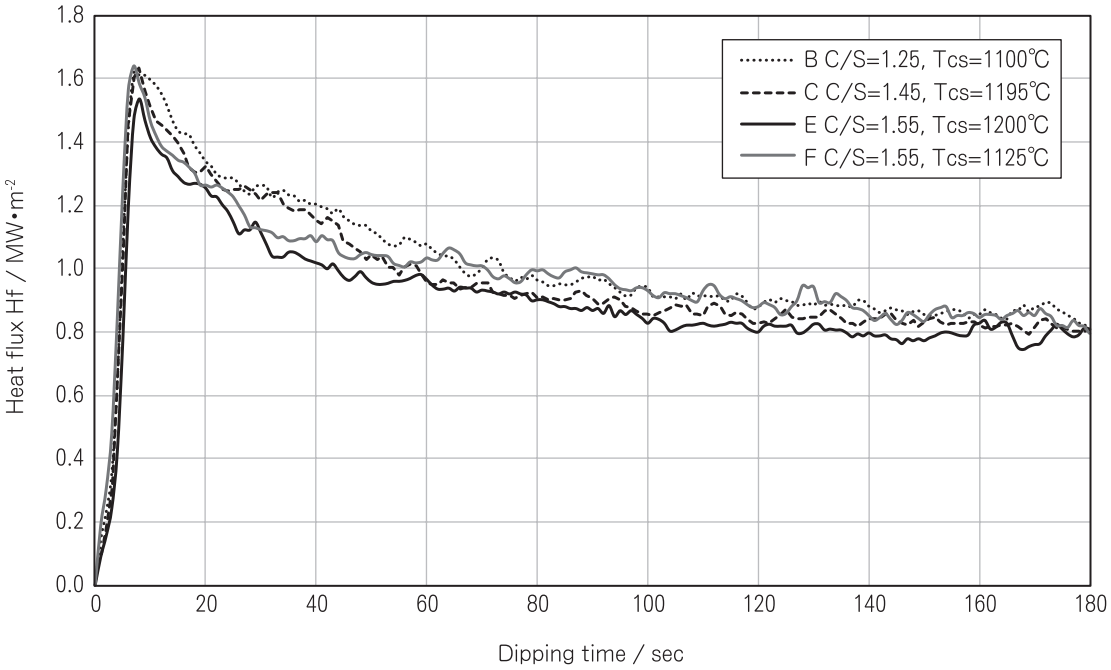

Fig.5 Heat flux in the slag film simulation test (C/S=basicity, Tsc=crystallization temp.).

by equation (1), which is obtained using the cooling water temperature difference between the inlet and the outlet in the stainless pipe.

$$Hf = c \cdot \rho w \cdot F \cdot \Delta T / A \quad \cdots\cdots (1)$$

Where, c is specific heat of water [$J \cdot kg^{-1} \cdot K^{-1}$] ρw is density of water [$kg \cdot m^{-3}$], F is cooling water rate [$m^3 \cdot s^{-1}$], ΔT is temperature difference of the inlet and the outlet [K], A is dipping area of the stainless pipe [m^2]. In the calculation; $c = 4.1868 \times 10^3$ and $\rho w = 1000$. The heat flux was increased immediately after the dipping, and it reached to the maximum point. After that, it gradually declined and became a steady state after 120 seconds. High basicity Samples E and F showed a large drop in heat flux after maximum point as compared with low basicity Samples B and C. Furthermore, for dipping times after 60 seconds, it was clearly shown that the heat flux of high crystallization temperature Sample E (1200 degree C) was lower than low crystallization temperature Sample F (1125 degree C).

Fig.6 shows the relationship between the crystallization temperature and the slag film thickness at 180 seconds. It was found that the slag film thickness increased as the crystallization temperature increased. According to the experiment results of slag film thickness formation and

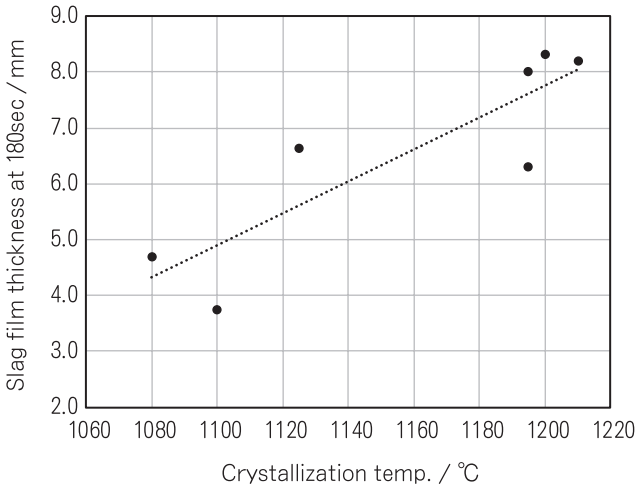

Fig.6 Relationship between slag film thickness at 180sec and crystallization temperature.

the behavior of heat flux, the crystal layer formation rate and heat flux before 60 seconds were influenced by the basicity. On the other hand, after 60 seconds, it was also observed that the influence of crystallization temperature on the crystal layer formation rate and heat flux was much larger than just sample basicity.

Fig.7 shows examples of the crystal structure observation results for the slag film formed on the stainless pipe surface. Because molten slag near the stainless pipe was

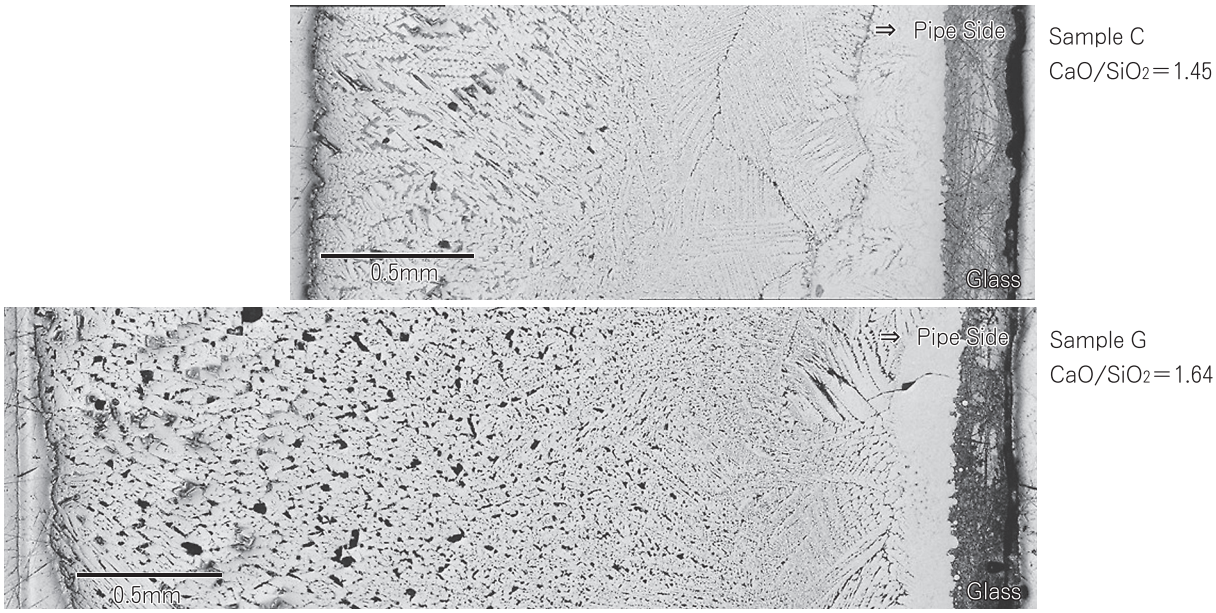

Fig.7 Cross section of slag films.

rapidly cooled after dipping, a glass layer was formed, and a fine crystal layer was formed outside the glass layer. As the distance from the stainless pipe surface increased, the dendritic crystal grain growth was greater. In addition, the crystal structure of the slag film obtained in this test was very similar to samples from the mold during actual casting. The molten slag side of the low basicity Sample C composed of fine acicular crystal grains. On the other hand, the high basicity Sample G was composed of coarse crystal grains, and since the solidification shrinkage amount was high, the rate of the pores (black portion) was increased.

2. 3 Discussion

In actual casting, molten slag flows into the gap between the mold and the steel shell from the meniscus with constant velocity as the cast strand withdraws, and the crystal layer in the slag film forms as it moves down the mold. In this process, it can be considered that the horizontal axis of Fig.3 represents the distance from the meniscus and the vertical axis of Fig.3 represents the thickness of crystallization layer. However, it should be noted that this interpretation can be used for the discussion of only the relative magnitude because there are differences between the actual casting and this consideration including no steel strand existence, slag film thickness, and heat removal condition. Fig.8 shows the relationships between distance from the meniscus and thickness of crystal layer profile. It was found that high basicity samples formed comparatively thicker crystal layer. Formation of the crystal layer can reduce total thermal conductivity by pores in the crystal layer[3], heat resistance of material interface, reducing heat radiation by opacity[14,15], and interfacial heat resistance caused by roughness of crystal layer surface on the mold wall[7]. Due to these factors, high basicity products can increase the thermal resistance in the meniscus area. This effect appeared to be confirmed based on the results of the heat flux in the slag film simulation test in Fig.5. In the slag film simulation test, high basicity samples showed a significant heat flux drop from the maximum point time to after 60 seconds. This should be due to the quick formation and growth of a crystal layer. Thus, the heat flux at the initial stage in this test, which means heat removal at the meniscus area in the actual casting, should be decreased by using high basicity mold powder. On the other hand, the heat flux of Sample E after around 60 seconds was lower than that of Sample F despite having the same basicity. This result might correspond to the crystallization layer of Sample E being thicker than that of Sample F, after around the 60 second mark in Fig.3. The difference between Samples E and F is the crystallization temperature. This might be associated with the fact that the crystal layer growth is slower. Mold powders with higher crystallization temperature tend to yield a

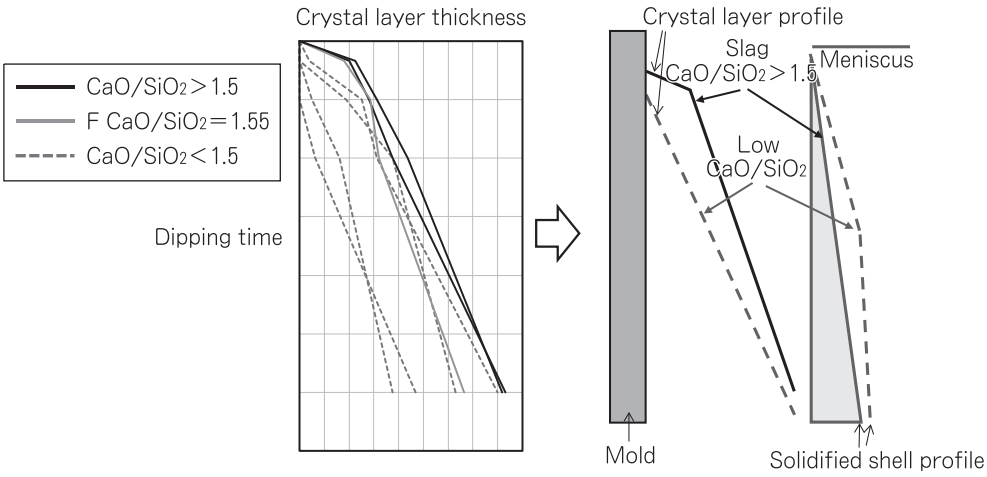

Fig.8 Image of crystal layer profile.

thicker crystal layer and provide lower heat transfer, this results in a decrease of the total thermal conductivity. As just described, because the crystallization temperature significantly affects the heat flux in moderate crystal layer growth over time, Fig.6 results suggest the total insulation property is influenced after certain period in the bottom part of the mold. The relationship between crystallization temperature and thickness of crystal layer can be explained by the distance and the temperature in the water cooled stainless pipe dipping into molten slag. The temperature gradient at the surface of water cooled stainless pipe can be considered almost equal after a certain period, thus it is more likely to form a crystal layer and complete solidification at the farther point of stainless pipe when the mold powder has a higher crystallization temperature. In the high speed casting conditions, forming a thinner crystal layer at bottom of the mold is effective in providing sufficient lubrication and maintaining solidified shell thickness. The thickness of the crystal layer should be decreased with a low crystallization temperature to gain this effect. In this development, basicity and crystallization temperature can be designed separately, like with Sample F in Fig.8, to arrange properties for various casting conditions.

3. Actual Casting Results

New high basicity mold powders were designed with the results and knowledge that were described in paragraph 2. The developed mold powders have been trialed on both a low speed casting (1.1m·min^{-1}) machine "Caster A", and a high speed casting (over 1.7m·min^{-1}) machine "Caster B". These trials were conducted on peritectic and medium carbon steel grades with carbon range were 0.08 to 0.18%.

3. 1 Trial result at Caster A

Fig.9 shows the thermocouple temperature profile results in the mold that were used to evaluate the mold powder basicity effect on powders with basicities of 1.2 and 1.8 on Caster A. The mold powder with a basicity 1.8 showed a lower temperature profile in upper position in the mold as compared with the powder with a lower 1.2 basicity. This result suggested that heat removal in meniscus area became softer with higher basicity. On the other hand, the lower position temperature profile of high basicity mold powder was detected to be higher than low basicity powder.

To evaluate and compare the mold heat flux property on the mold broad face, heat flux Hw [W·m^{-2}] was calculated by equation (2) that using the temperature difference of mold cooling water between inlet and outlet. Fig.10 shows the calculated results for the mold heat flux of each mold powder.

Where, c is specific heat of water [J·kg^{-1}·K^{-1}], ρw is water density [kg·m^{-3}], Fw is cooling water flow rate of mold broad face [m^3·s^{-1}], ΔTw is temperature difference of mold cooling water through the broad face between inlet and outlet [K], Lw is mold width length [m], and Lm is mold vertical effective length [m], which is from molten steel meniscus to mold bottom end. In the calculation, c=4.1868×10^3 and ρw =1000 were used.

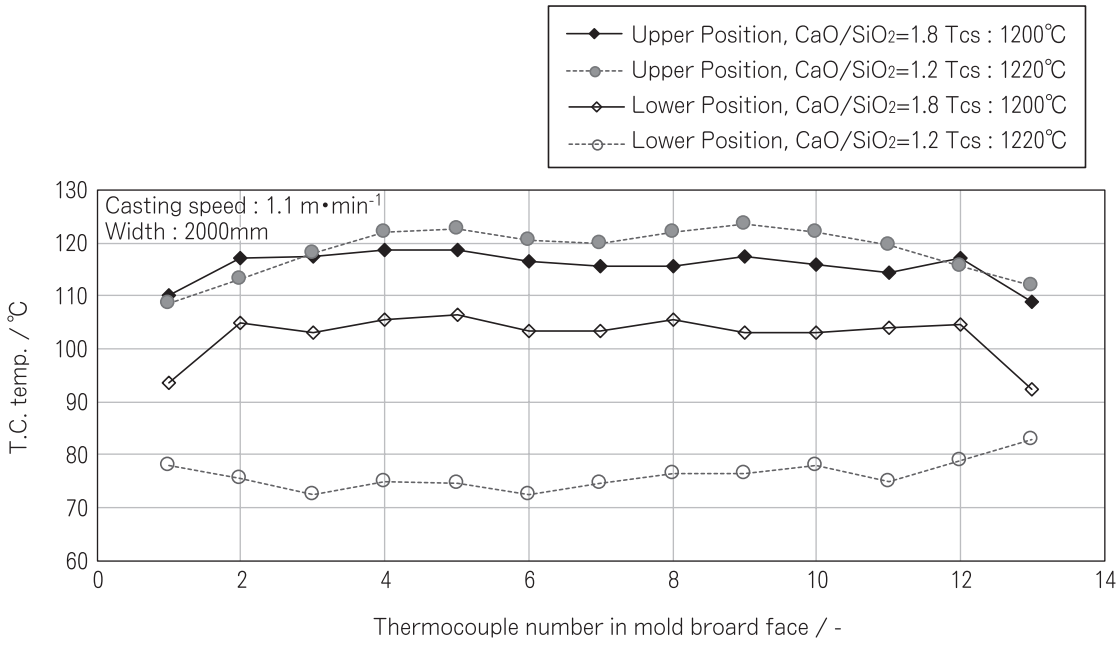

Fig.9 Thermocouple temperature profile in themold (Tcs=crystallization temp.).

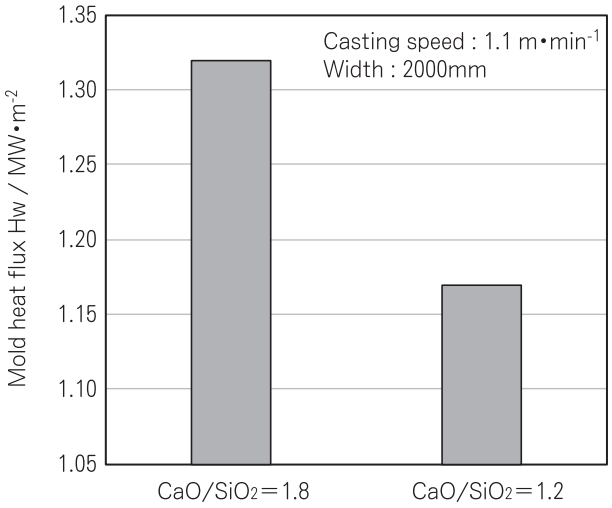

Fig.10 Mold heat flux.

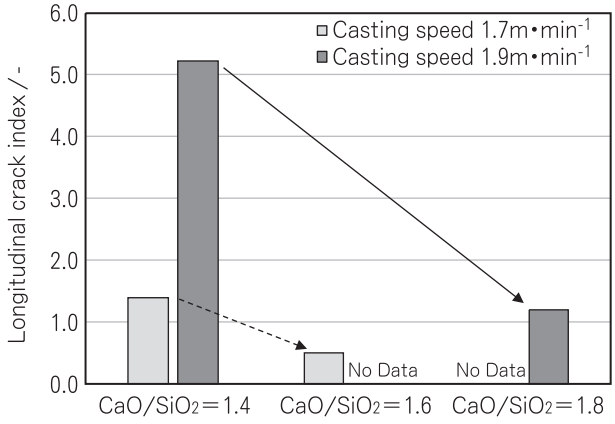

Fig.11 Longitudinal crack results.

The mold heat flux of developed high basicity mold powder was higher than that of low basicity type.

$$Hw = c \cdot \rho w \cdot Fw \cdot \Delta Tw / (Lw \cdot Lm) \quad \cdots\cdots (2)$$

3. 2 Trial result at Caster B

Fig.11 shows longitudinal cracking results for 1.4, 1.6, and 1.8 basicity mold powder trials at Caster B. When using a conventional mold powder with a basicity of 1.4, longitudinal cracks increased significantly when casting speed was greater than 1.9m/min, whereas the newly developed high basicity powders yielded a low occurrence longitudinal cracks when casting in the higher speed range. In addition, it was observed that heat removal was sufficient to maintain solidified steel shell thickness that was required for the higher speed casting.

To consider the heat removal behavior in the mold, the heat flux of the mold broad face (Hw) when using various mold powders was investigated. Fig.12 shows the relationship between calculated Hw by equation (2) and the casting speed. The basicity of the mold powders was designed to be in the range of 1.4 to 2.0, and the

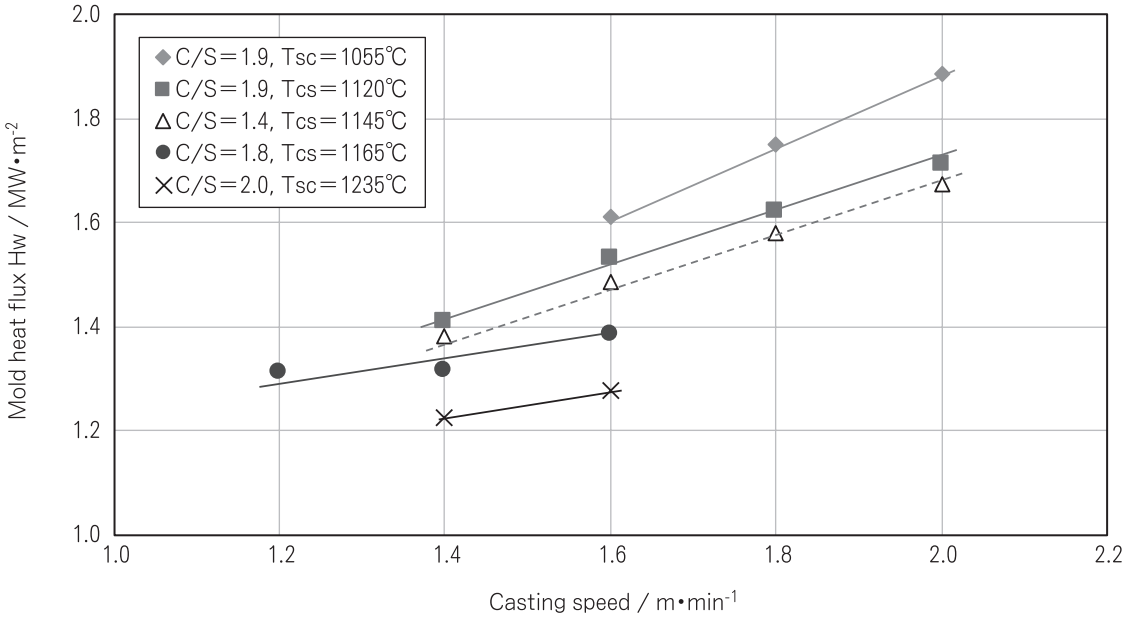

Fig.12 Relationship of mold heat flux and casting speed (C/S=basicity, Tcs=crystallization temp.).

crystallization temperature was adjusted with chemical compositions of various fluxes. Slag viscosity at 1300 degree C was set in the range of 0.05Pa·s to 0.06Pa·s for each mold powder.

It was determined that mold heat flux had a strong correlation with crystallization temperature instead of basicity.

3. 3 Application of developed high basicity mold powders

Fig.13 shows the application of the developed high basicity mold powders on medium carbon grades. The developed mold powders, which have optimal crystallization, have achieved stable casting and improved steel quality. They are widely used today from low to high casting speed conditions.

3. 4 Summary of actual casting test result

When casting, the upper position thermocouple temperature profile results in Fig.9 suggested that the newly developed high basicity mold powders have an optimal crystallization temperature sufficient to form an effective crystal layer in the meniscus area. On the other hand, the lower position thermocouple temperature results showed an opposite tendency; that the developed high basicity result provided a higher temperature than that of lower basicity mold powder. The results suggest that the developed mold powder has higher heat removal ability in the lower part of the mold. In addition, the result of

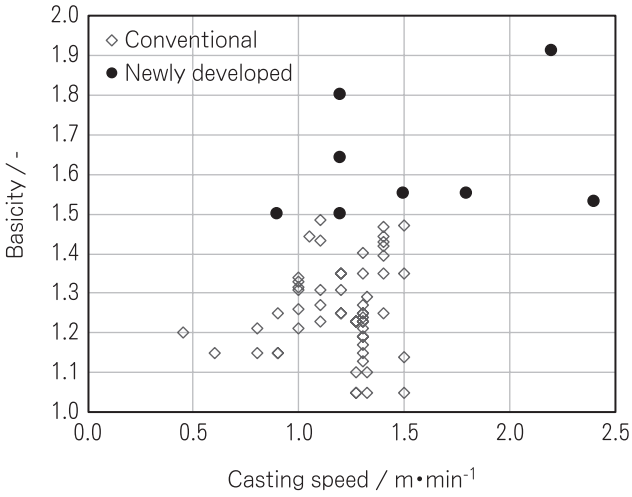

Fig.13 Mold powder application matrix in casting speed and basicity on medium carbon steel casting.

thermocouple temperature profile in Fig.9 suggests that a short dipping time in the slag film simulator test can simulate the crystallization behavior of mold powder in meniscus area even though it is relative.

According to the results shown in Fig.11, higher basicity can prevent the cracks at a casting speed of 1.9m·min^{-1}. Additionally, it was demonstrated that preventing the origin of uneven solidification through softer heat removal in the meniscus area is effective in preventing the cracks.

The results of Fig.10 and Fig.12 suggests that total heat removal in actual mold is strongly affected by the crystallization temperature. Even though the high basicity mold powder has a higher crystal layer formation rate, optimizing the crystallization temperature will provide the heat removal needed to maintain solidified shell thickness in the lower part of the mold. Moreover, the results obtained by actual casting indicats that the slag film simulation test is a useful way to evaluate the crystallization behavior and heat removal characteristics in the development of the mold powder.

4. Conclusions

In this development, we recognized that the increased crystal layer formation rate in the slag film which accompanies higher basicity was able to give softer heat removal in meniscus area and optimize heat removal in the lower part of the mold. This is possible due to crystallization temperature control. This technology has prevented some types of cracks while maintaining stable casting operation. The new knowledges gained from this development are:

1） Developed a new slag film simulation test that is very useful in the development of mold powder.
2） According to the slag film simulation test results, the crystal layer formation rate was increased significantly for mold powder with a basicity ≥ 1.55.
3） The newly developed high basicity mold powder yielded softer heat removal in meniscus area by increasing the crystal layer formation rate through higher basicity. Additionally, in the lower part of the mold, sufficient heat removal was maintained to form adequate solidified shell thickness by means of crystallization temperature control. The newly developed mold powder can control the crystal layer formation rate and crystallization temperature separately.
4） When trialed, the newly developed high basicity mold powder has reduced surface cracks on the strand surface. In addition, it was also more effective in improving steel surface quality in high-speed casting applications.

References

1） Y. Sugitani and M. Nakamura : Tetsu-to-Hagané, **65** [1] 42–51 (1979).
2） T. Kanazawa, S. Hirai, M. Kawamoto, K. Nakai, K. Hanazaki and T. Murakami : Tetsu-to-Hagané, **83** [11] 701–706 (1997).
3） T. Chikano, K. Ichikawa and O. Nomura : Shinagawa Technical Report, [31] 75–84 (1988).
4） T. J. H. Billany, A.S. Normanton, K.C. Mills and P. Grievenson : Ironmaking and Steelmaking, **18** [6] 403–410 (1991).
5） K. Ichikawa, A. Morita and Y. Kawabe : Shinagawa Technical Report, [36] 99–108 (1993).
6） S. Ogibayashi and T. Mizoguchi : CAMP–ISIJ, **7** [4] 1154 (1994).
7） K. Watanabe, S. Suzuki, K. Murakami, H. Kondo, A. Miyamoto and T. Shiomi : Tetsu-To-Hagané, **83** [2] 115–120 (1997).
8） H. Shibata, K. Kondo, M. Suzuki and T. Emi : ISIJ International, **36** S179–S182 (1996).
9） E. Nakatani, H. Ogata, T. Suzuki, S. Takeuchi, Y. Hoshiyama and S. Takanaga : Taikabutsu, **67**, [8] 388–391 (2015).
10） M. Hanao, M. Kawamoto and T. Watanabe : ISIJ International, **44**, [5] 827–835 (2004).
11） M. Hanao, M. Kawamoto, M. Hara, T. Murakami, H. Kikuchi and K. Hanazaki : Tetsu-to-Hagané, **88** [1] 23–28 (2002).
12） A. Morita, T. Omoto, M. Shinkai, H. Amano and T. Kashima : Shinagawa Technical Report, [41] 53–64 (1998).
13） T. Omoto, H. Ogata and J. Ito : Shinagawa Technical Report, [49] 73–76 (2006).
14） S. Ohmiya, K. H. Tacke and K. Schwerdtfeger : Ironmaking and Steelmaking, **10** [1] 24–30 (1983).
15） A. Yamauchi, K. Sorimachi, T. Sakuraya and T. Fujii : Tetsu-to-Hagané, **79** [2] 167–174 (1993).